Damage-based strength reduction factor for nonlinear structures subjected to sequence-type ground motions

Yongqun Zhang[a], Jun Chen[a,b,*], Chaoxu Sun[a]

[a] Department of Structural Engineering, College of Civil Engineering, Tongji University, Shanghai, PR China
[b] State Key Laboratory of Disaster Reduction in Civil Engineering, Tongji University, Shanghai, PR China

ARTICLE INFO

ABSTRACT

This paper investigates the strength reduction factor of single-degree-of-freedom (SDOF) system subjected to the mainshock–aftershock sequence-type ground motions. Both displacement ductility and cumulative damage are considered in the reduction factor. Records of mainshock-aftershock earthquakes were collected and classified according to site properties. The aftershock ground motions in sequence are scaled to five relative intensity levels. Based on the nonlinear time-history analysis of inelastic SDOF systems, the effects of natural period, ductility factor, damage index and aftershock have been studied statistically. The results indicate that the aftershock ground motion has significant influences on strength reduction factors, and the damage-based strength reduction factor is about 0.6−0.9 times of the ductility-based strength reduction factor. Finally, an empirical expression for strength reduction factor was established by regression analysis.

1. Introduction

According to statistics, about 88% of strong earthquakes are accompanied by aftershocks. An aftershock is defined as a smaller earthquake following the mainshock, which is the largest earthquake in the sequence. Structural damage caused by the mainshock is further aggravated under aftershocks and can even lead to structural collapse. The 2010 New Zealand [1] and the 2015 Nepal earthquakes [2] experienced both mainshock and aftershock ground motions, and are good examples of why sequence-type ground motions are important issues at the structural design stage. In recent years, researchers have explored the effect of aftershock from different aspects. Some studies explored the effects of sequence-type ground motions on inelastic spectra such as strength reduction factor spectra [3,4], damage spectra [5], ductility factor spectra [6,7], etc. Others focused on the changes of structural response, e.g. steel frame buildings [8] and RC frames [9], under sequence-type ground motions. All the results clearly show larger peak displacement or increased structural damage due to sequence-type ground motions than that of one major earthquake. The effect of aftershock should not be overlooked at the structural design stage.

Current seismic design principles include analysis of a structure's elastic-plastic behavior under moderate/rare earthquakes. Since the design strength of most structures is generally much

lower than the minimum strength required to maintain the elastic stage under strong earthquakes, a reduction factor is often used to reduce the elastic strength demand and thereby obtain the elastic-plastic strength demand of a structure. Theoretical analysis and experimental studies of strength reduction factors have demonstrated that the structure ductility has a significant effect on the strength reduction factor. The displacement ductility factor helps to assess the extent of structural damage [10−12]. Therefore, a ductility-based strength reduction factor R_μ can be defined as:

$$R_\mu = \frac{F_e}{F_{y,\mu}} = \frac{F_y(\mu = 1)}{F_y(\mu = \mu_i)} \tag{1}$$

where $F_y(\mu=1)$ is the yield strength required to maintain the structure in elastic stage; $F_y(\mu=\mu_i)$ is the yield strength required to maintain the ductility demand of the structure equal to a given target ductility value as μ_i.

Moreover, the cumulative damage of nonlinear hysteresis cycles also plays a significant role in determining the damage level of a structure. Some studies suggest that cumulative damage can be accounted for by modifying the ductility capacity, such as the equivalent ductility method [13] or introducing a weighted ductility factor [14]. These methods indirectly take into account the influence of cumulative damage. Some other studies consider the cumulative damage directly by employing a damage model in the determination of the seismic demand for a given damage level or performance level.

---

* Corresponding author at: Department of Structural Engineering, College of Civil Engineering, Tongji University, Shanghai, PR China.
E-mail address: cejchen@tongji.edu.cn (J. Chen).

Table 1
Number of recorded sequence-type ground motions used in this paper.

Earthquake name	Mainshock		Aftershock		Number	
	Time	M_W	Time	M_W	Site B	Site C
Managua, Nicaragua	1972/12/23 06:29	6.2	1972/12/23 07:19	5.2	0	2
Imperial Valley	1979/10/15 23:16	6.5	1979/10/15 23:19	5.0	0	26
Mammoth Lakes	1980/05/25 16:34	6.1	1980/05/25 16:49	5.7	2	4
Coalinga	1983/05/02 23:42	6.4	1983/05/09 02:49	5.1	0	2
Whittier Narrows	1987/10/01 14:42	6.0	1987/10/04 10:59	5.3	6	14
Superstition Hills	1987/11/24 05:14	6.2	1987/11/24 13:16	6.5	0	2
Northridge	1994/01/17 12:31	6.7	1994/01/17 12:32	6.1	14	13
Umbria Marche	1997/09/26 09:44	6.0	1997/10/03 08:55	5.3	8	4
Chichi	1999/09/20	7.6	1999/09/20 17:57	5.9	49	36
Wenchuan	2008/05/12 14:28	7.9	2008/05/12 19:11	6.1	12	7
L'Aquila	2009/04/06 01:33	6.3	2009/04/07 17:47	5.6	9	0
New Zealand	2010/09/03 16:35	7.0	2011/02/21 23:51	6.2	9	33
East Japan Earthquake	2011/03/11 13:46	9.0	2011/03/11 15:15	7.7	34	29
Kumamoto	2016/04/14 21:26	6.2	2016/04/16 01:25	7.0	11	16
				Total	154	188

Table 2
Damage index ranges for different performance levels.

Performance level	Degree of damage	Damage index range
Operational	Negligible	0 < D < 0.1
Immediate occupancy	Minor	0.1 < D < 0.2
Damage control	Moderate	0.2 < D < 0.5
Life safety	Severe	0.5 < D < 0.8
Collapse prevention	Near collapse	0.8 < D < 1.0
Loss of building	Collapse	1.0 < D

The strength reduction factor obtained in this way is therefore referred to as a damage-based strength reduction factor R_D [15], which can be written as:

$$R_D = \frac{F_e}{F_{y,D}} = \frac{F_y(\mu = 1, D = 0)}{F_y(\mu = \mu_i, D = D_j)} \qquad (2)$$

where $F_{y,D}$ is the inelastic strength demand to limit the inelastic response of the structure to a specified damage level D_j for a given ductility capacity μ_i. In this study, the performance levels of a structure are defined using a damage index to take the cumulative damage of the structure into consideration.

As mentioned above that the aftershock will aggravate structural damage, current damage-based strength reduction factor, however, does not reflect the influence of aftershock ground motions. In this regard, the current study explores this issue through extensive numerical calculations on a nonlinear SDOF system subjected to sequence-type ground motions. Section 2 collects real mainshock and aftershock ground motion records that are essential to investigate R_D. The collected records are then divided into different categories according to the site condition. Section 3 defines the

performance level and computational parameters to be used in the calculation of R_D. In Section 4, extensive elastic-plastic time history analysis of a nonlinear SDOF system with various parameters are then carried out to determine the R_D for two cases, i.e., mainshock only and mainshock plus one aftershock. The influence of ductility factor, damage index and some other parameters on R_D are explored in Section 5 through parametric studies. Finally, an empirical formula for damage-based strength reduction factor is proposed in Section 6.

2. Records and classification of sequence-type ground motions

A sequence-type ground motion record usually consists of one mainshock event and one or multiple aftershock events, which are called as one earthquake (mainshock only), a sequence of two earthquakes (mainshock plus one aftershock), a sequence of three earthquakes (mainshock plus two aftershocks), and so on. Scenario of mainshock plus one aftershock was commonly considered in previous studies [5,7,8]. Their results demonstrated that two-sequence earthquakes can provide valuable information about the influence of aftershock. Therefore, sequence-type ground motion in this study is specified as one mainshock plus one aftershock.

To build up a ground motion of two earthquake events, one can connect two artificial ground motions [5] or connect a real earthquake record with its duplicate [16]. This usage of artificial ground motions, however, might lead to significant overestimation of maximum lateral drift demands [17]. The degree of overestimation is case-based due to the random nature of artificial ground motion simulation. The repeated earthquake methodology, on the other hand, actually assumes that the mainshock and aftershock have same power spectrum density which may not be tenable for real situation. To avoid the above problems, this study uses real earthquake records available in Pacific Earthquake Engineering Research Center (PEER) [18] and Strong-motion seismograph networks (K-NET, KiK-net) [19] to construct sequence-type ground motion by the following steps and criteria: (1) collect records from seismostations located on free-field or low-rise buildings to avoid possible soil-structure interaction effects; (2) among all the records from same station and same earthquake event, the one happening earlier and having a peak ground acceleration (PGA) larger than $0.10g$ is taken as the mainshock, the one having the second largest PGA and larger than $0.05g$ is taken as the aftershock; (3) the earthquake magnitude of mainshock and aftershock is larger than 6.0 and 5.0, respectively; (4) connect the selected mainshock and aftershock with a time gap of 100 s in between, which is long enough to cease structural vibrations caused by mainshock; (5) classify the connected sequence-type ground motion according to site classification method of United States Geological Survey.

In total, we constructed 342 sequence-type ground motion records for site classes B and C as listed in Table 1. The number of qualified records for site classes A and D are too small to conduct any meaningful statistical analysis. For further analysis, the PGA of mainshock of all the selected sequence-type ground motion records were scaled to an identical value of $0.2g$.

The relative peak ground acceleration of aftershock ground motion γ is defined as:

$$\gamma = \frac{PGA_{as}}{PGA_{ms}} \qquad (3)$$

where PGA_{as} is the PGA of aftershock ground motion, PGA_{ms} is the PGA of mainshock ground motion. The parameter γ was introduced to represent the relative intensity level of aftershock with respect to the mainshock. The intensity of aftershock is usually smaller than that of mainshock. However, the aftershock ground motions with greater intensity with respect to that of mainshock ground motions do exist
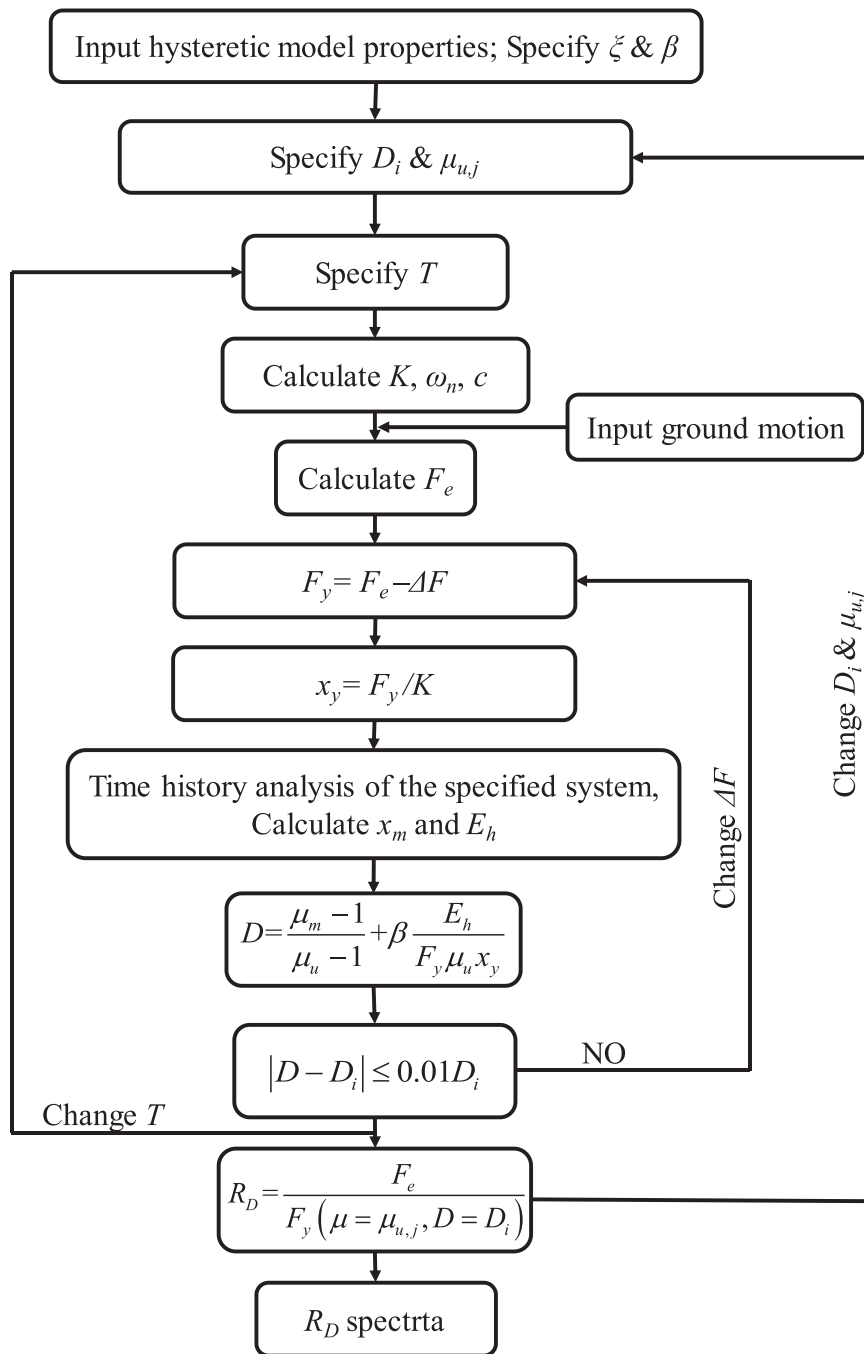
Fig. 1. The flowchart for the computation of R_D factor.

in real earthquake records. Thus, to study the effect of relative intensity of aftershock on the strength reduction factor, five levels of γ are considered in this study, there are γ=0.5, 0.8, 1.0, 1.2 and 1.5.
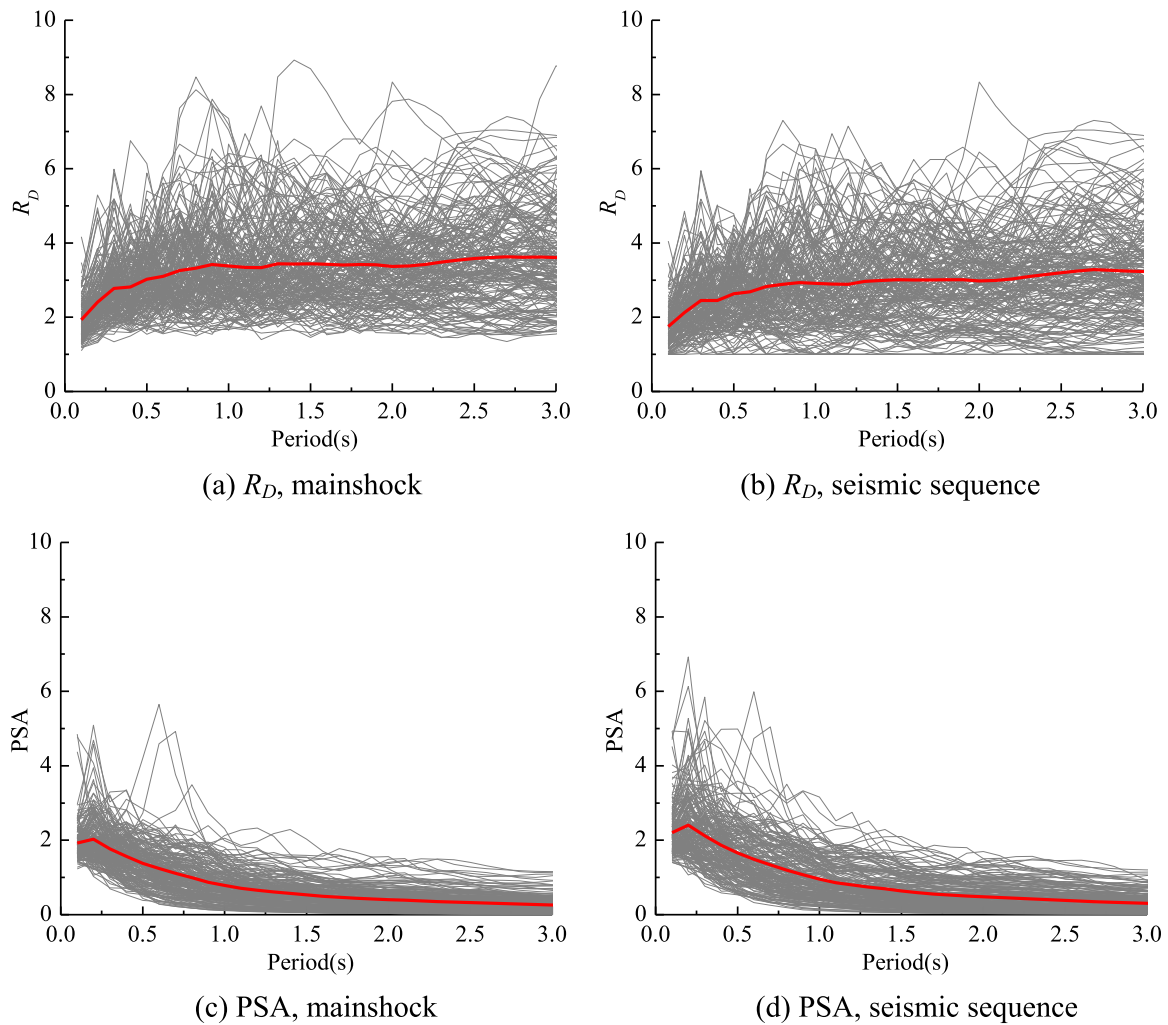
3. Computational parameters and procedures

3.1. Definition of performance level and corresponding limit values

Peak displacement or storey drift are common parameters used in performance levels in performance-based structural design and evaluation. However, structural damage takes on various forms

under an earthquake, and the extent of the structural damage may not be fully reflected by maximum deformation or storey drift only [20,21]. That's why reasonable indicators must be used to assess the extent of structural damage. The maximum deformation of a structure and its hysteretic energy are the main factors for quantifying structural damage. Based on the well-known Park-Ang model [22], the modified model proposed by Kunnath et al. [23] is employed here to assess the damage of structures, which is

$$D = \frac{\mu_m - 1}{\mu_u - 1} + \beta \frac{E_h}{F_y \mu_u x_y} \qquad (4)$$

(a) R_D, mainshock

(b) R_D, seismic sequence

(c) PSA, mainshock

(d) PSA, seismic sequence

Fig. 2. Pseudo spectral accelerations (PSA) and R_D factor (Site class C, D=1.0, μ_u=6). (a) R_D, mainshock (b) R_D, seismic sequence (c) PSA, mainshock (d) PSA, seismic sequence.

where D is the damage index, μ_m is the ductility factor when the structure reaches the maximum elastic-plastic deformation under earthquake ground motion, μ_u is the ductility factor when the structure fails under monotonic loading, F_y is the yield strength, x_y is the yield displacement, E_h is the cumulative hysteretic energy dissipation under earthquake ground motion, β is a constant parameter that represents the ratio of cumulative damage caused by hysteretic energy. Negro [24] evaluated the typical β values concerning the global behavior of structures through experimental assessment. For a structure with high ductility, β should take lower value, and vice versa. In this study, β is taken as 0.1 to represent a basic ductile design.

To associate the performance levels with the damage index resulting from modified Park-Ang model, performance levels and the range of the damage index should be determined firstly. Four performance levels, namely *Operational*, *Immediate Occupancy*, *Life Safety* and *Collapse Prevention*, are proposed by FEMA-356 [25] to describe the structural damage states. A large collection of observed seismic structural damage, which are used to calibrate the damage index in Eq. (4), show that D=(0.2–0.5) is the boundary of repairable damage and unrepairable damage while the D approaching 0 represents elasticity without damage. Thus, an additional performance level named *Damage Control* was suggested between *Immediate Occupancy* and *Life Safety* [26]. The ranges of the damage indices

for each performance level are listed in Table 2.

### 3.2. Analysis method and structural parameters

The dynamic equilibrium equation of a nonlinear SDOF system subjected to an earthquake is given by:

$$m\ddot{x} + c\dot{x} + f_s = -m\ddot{x}_g \qquad (5)$$

where c is the damping coefficient; f_s is the restoring force of the structure; x is the relative displacement, and x_g is the ground displacement.

According to the definition of the strength reduction factor in Eq. (2), it is able to calculate the R_D spectra by Eq. (5) when the period, damping ratio and restoring force model of the SDOF system are given. Fig. 1 shows the computation flowchart for determining R_D spectra. For any ground motion input, the R_D is calculated by gradually reducing the strength ΔF from the corresponding elastic strength F_e under given ductility until the specified D is achieved within a tolerance of 1%. Then, a series of strength reduction factors R_D for SDOF system in different ductility factors μ_i and damage indexes D_j can be obtained by calculating different periods and ground motions, which constitute the R_D spectra.
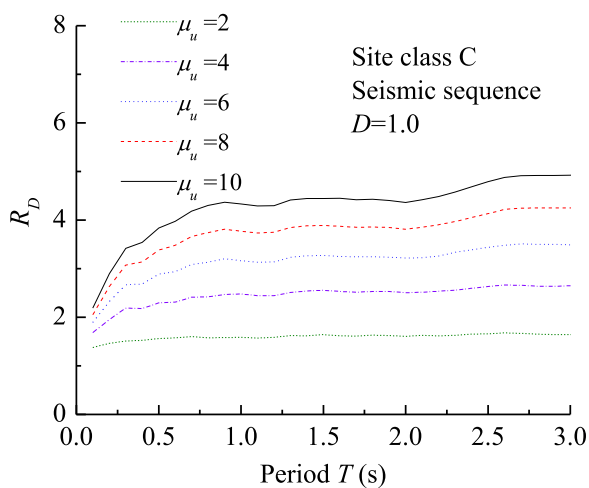
For a comprehensive study of the R_D factor under single earthquakes and sequence-type earthquakes, a series of SDOF systems are employed in the calculation. The hysteretic model used in this study is
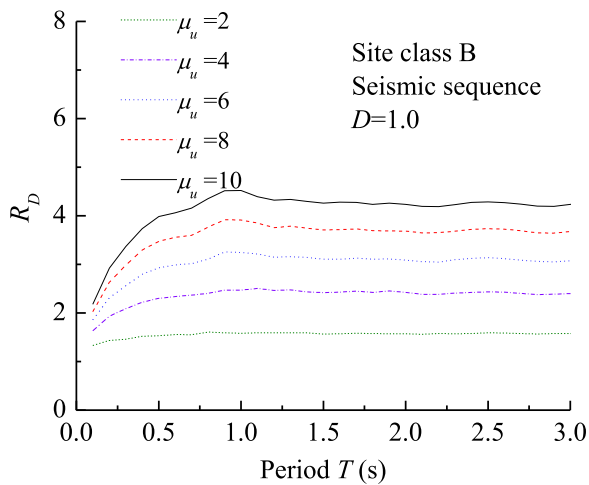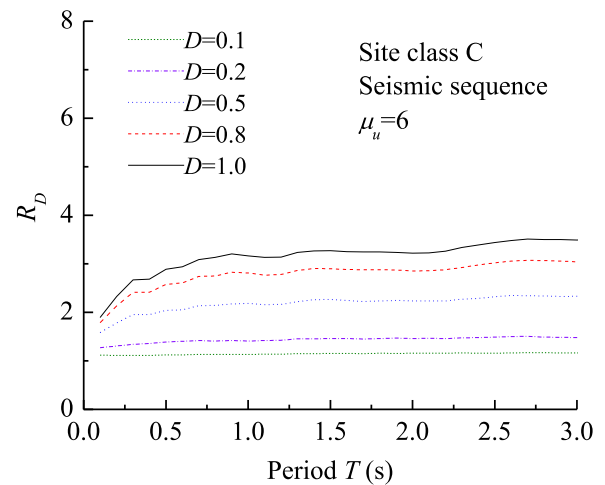
(a) R_D factor on site class B
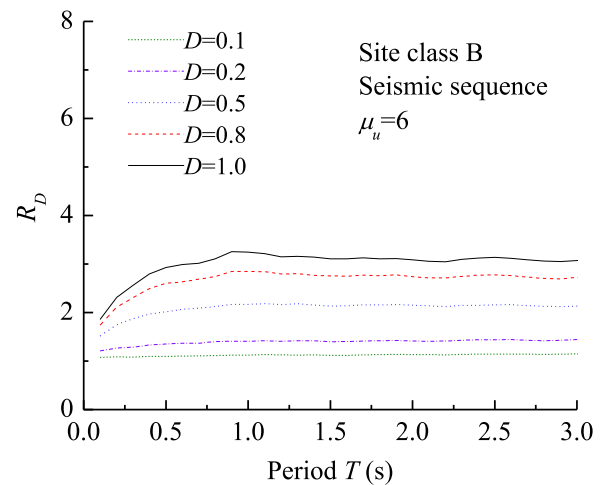
(a) R_D factor on site class B

(b) R_D factor on site class C

(b) R_D factor on site class C

Fig. 3. Influence of ductility on R_D factor, D=1.0, γ=0.5. (a) R_D factor on site class B (b) R_D factor on site class C.

Fig. 4. Influence of damage index on R_D factor, μ_u=6, γ=0.5. (a) R_D factor on site class B (b) R_D factor on site class C.

elastic-perfectly plastic model because of its simple constitutive relationship. The natural period of the SDOF system varied from 0.1 to 3.0 s with an interval of 0.1 s and its viscous damping ratio was assumed to be 5%. Five ductility factors μ=2, 4, 6, 8 and 10 are selected to consider the different ductility performance, and five damage indices D=0.1, 0.2, 0.5, 0.8 and 1.0 are selected to consider the different damage level.

4. Mean strength reduction factors

Using the procedure just described, a total of 513,000 strength reduction factors are computed, corresponding to the SDOF systems with 30 periods undergoing five different levels of ductility and five levels of damage index when subjected to 342 mainshock ground motions and corresponding 342 main-aftershock ground motions. Results are analyzed statistically according to the period, the ductility, the damage index of the system and the site condition where the motion is recorded. For example, Fig. 2 shows all the calculated R_D curves and pseudo spectral accelerations (PSA) curves for μ=6, D=1.0 and site class C for mainshock and seismic sequence, respectively. Their mean spectra are also plotted in thick

solid lines. Due to space limited, just the representative results are shown in the following sections, while other cases having the similar results are not shown.

The mean R_D spectra of the SDOF systems of different ductility classes and damage indices for the two site classes subjected to mainshock ground motions and mainshock-aftershock ground motions with γ=0.5 are shown in Figs. 3 and 4. As shown in the figures, the R_D factor shows the same trend regardless of ductility, damage index, site condition and type of ground motions. The R_D factor increases with increasing period of systems, the variation is dramatical in short period region (0–1.0 s). In the long period region (1.0–3.0 s), the R_D factor is approximately period independent and approach to a constant value based on ductility and damage index.

For a given damage index, the mean R_D increases with the increase of ductility factor. That is to say, the strength demand of the structures with high ductility is smaller than that of the structures with poor ductility. It indicates that structures with sufficient ductility can withstand a certain degree of damage caused by earthquake. The ductility has significant effect on the R_D. For example, the average difference between the mean R_D of μ=2 and 4 is about 34% for the structures with D=1.0 on site class B subjected to sequence-type ground motions.
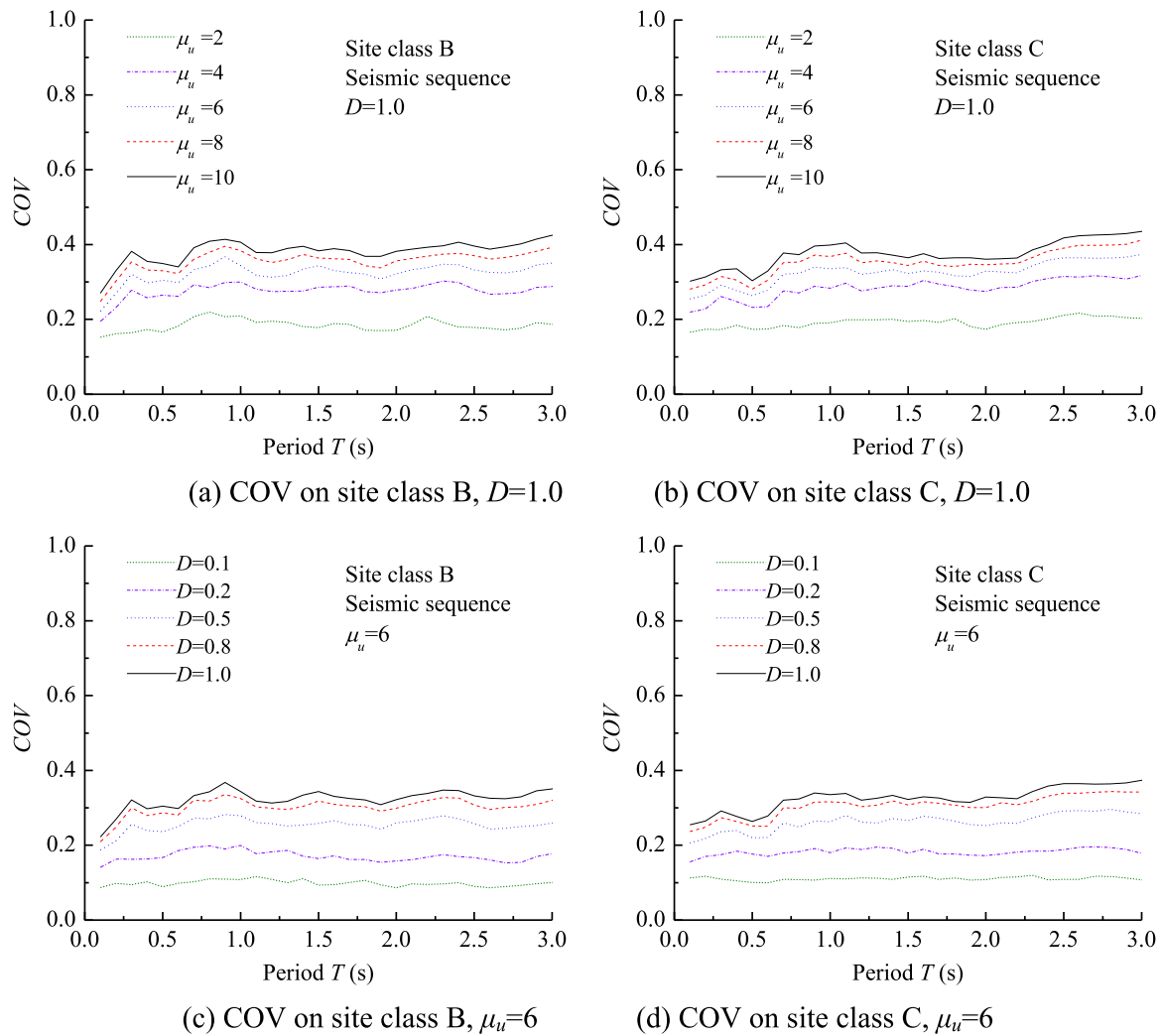
(a) COV on site class B, D=1.0

(b) COV on site class C, D=1.0

(c) COV on site class B, μ_u=6

(d) COV on site class C, μ_u=6

Fig. 5. The COVs of mean R_D factor, γ=0.5. (a) COV on site class B, D=1.0 (b) COV on site class C, D=1.0 (c) COV on site class B, μ_u =6 (d) COV on site class C, μ_u=6.

For a given ductility factor, the mean R_D increases with the increase of target damage index. It indicates that the damage of the structure with high strength is lighter than that of the structure with low strength subjected to same ground motion. The effect of damage index is considerable. For example, the average difference between the mean R_D of D=0.2 and 0.5 is about 31% for the structures with μ=6 on site class B subjected to sequence-type ground motions.

To reflect the degree of dispersion of the strength reduction factor spectra, the coefficients of variation (COV) of the corresponding mean R_D spectra are calculated, the COVs of R_D spectra subjected to sequence-type ground motions with γ=0.5 are shown in Fig. 5. The COV is defined as the ratio of the standard deviation to the mean.
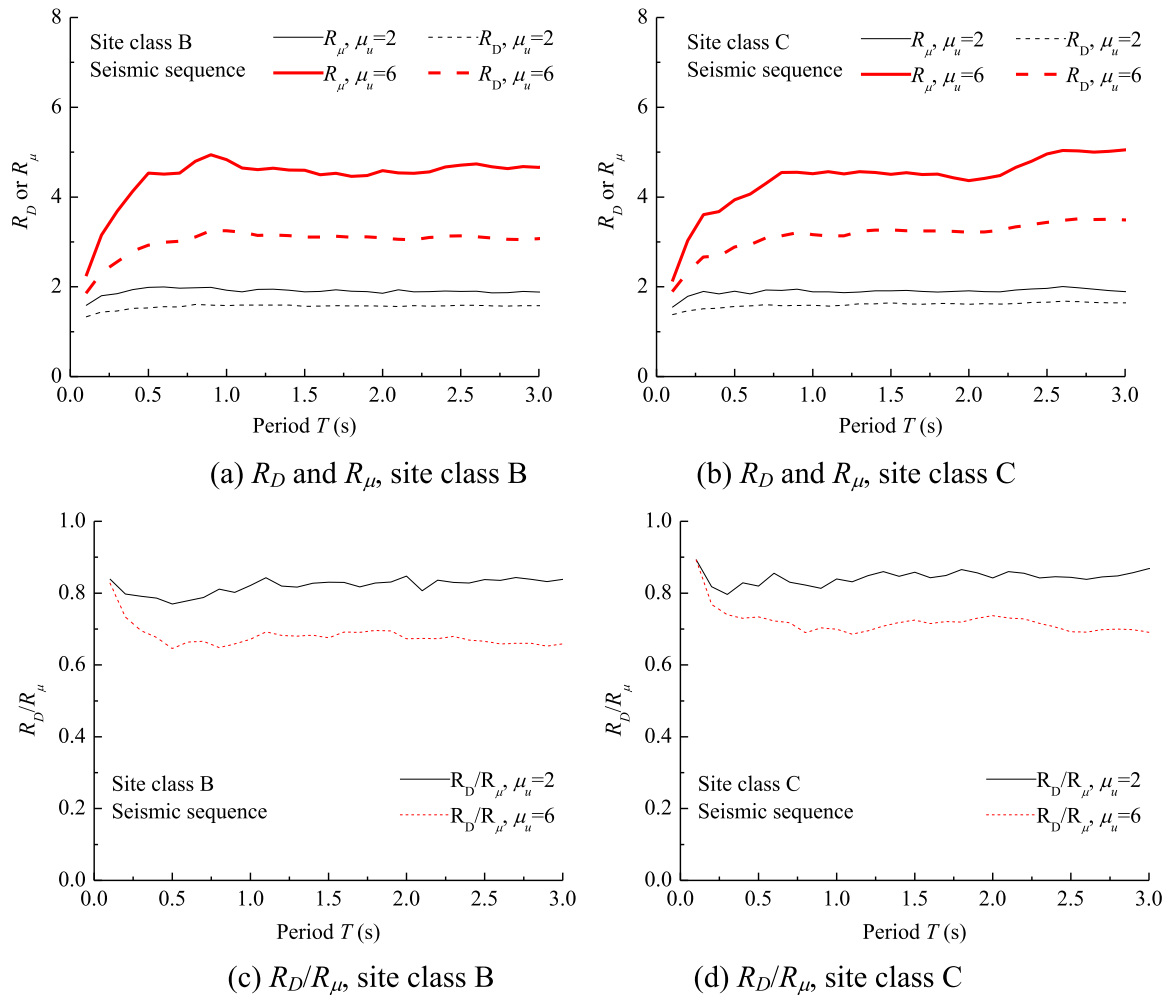
The COVs are independent of the period, and COVs on different site class present the approximate trend. However, for a given period, the COVs change rapidly with the variation of damage index and ductility factor. The maximum coefficient of variation of the mean strength reduction factor calculated under each group site condition does not exceed 45%, which reflects the randomness and discreteness of the ground motion in a certain extent.

In order to study the influence of the cumulative damage on the strength reduction factor, the assessment of structural damage

parameters using displacement and modified Park-Ang damage index respectively are compared, and the difference of the ductility-based strength factor R_μ and the damage-based strength factor R_D is calculated under the same sequence-type ground motions, as shown in Fig. 6. When the damage index and the ductility factor are same, R_μ and R_D changing with period of structure are mainly the same. Because of the damage contribution in terms of energy, the displacement demand of R_D is less than that of R_μ, so the R_D value is always less than the R_μ value. Under sequence-type ground motions, the ratio between the R_D and R_μ is 0.8–0.9 for low ductility factor (μ=2), and the ratio is 0.6–0.9 for high ductility factor (μ=6).

In the short period region, the mean R_D/R_μ for sequence-type ground motions with γ=0.5 decreases drastically with the period increases, indicating that the effect of energy item accounts in damage index is changed rapidly. Because the yield strength of system is large when period is close to zero, the hysteretic energy dissipation is small relatively, thus the difference of R_D and R_μ is small. The yield strength of system decreases and the hysteretic energy dissipation increases when period increases, so the changing of R_D is more greatly than R_μ and the R_D/R_μ decreases drastically.

In the long period region, the mean R_D/R_μ for sequence-type ground motions with γ=0.5 decreases slightly with the period increases.

(a) R_D and R_μ, site class B

(b) R_D and R_μ, site class C

(c) R_D/R_μ, site class B

(d) R_D/R_μ, site class C

Fig. 6. Comparison between R_D (damage-based, D =1.0) and R_μ (ductility-based) spectra, γ=0.5. (a) R_D and R_μ, site class B (b) R_D and R_μ, site class C (c) R_D/R_μ, site class B (d) R_D/R_μ, site class C.

The yield strength and yield displacement decrease weakly and the energy item accounts in damage index increases slightly with the period increases.

5. Influence of various parameters

5.1. Effect of aftershock on the R_D spectra

To evaluate the effect of aftershock on the R_D factors, the value of $R_{D,\,seq}/R_{D,\,ms}$, which represents the ratio between R_D of sequence-type ground motions (denoted as $R_{D,\,seq}$) and corresponding R_D of mainshock ground motions ($R_{D,\,ms}$), are employed. The mean $R_{D,\,seq}/R_{D,\,ms}$ is calculated with the structures of different ductility factors and damage indices subjected to different intensity of aftershock, part of the results are shown in Figs. 7–9.

Fig. 7 shows the mean $R_{D,\,seq}/R_{D,\,ms}$ for sequence-type ground motions with γ=0.5 and μ=6 (Fig. 7a and c), and for γ=0.5 and D=1.0 (Fig. 7b and d). The mean $R_{D,\,seq}/R_{D,\,ms}$ are within [0.94, 0.98] Ce within [0.93, 0.99] on site class C. The difference between $R_{D,\,seq}$ and $R_{D,\,ms}$ is less than 10%, so the aftershock ground motions with γ=0.5 can be ignored in evaluating the R_D factor.

When γ increase to 1.0, the mean $R_{D,\,seq}/R_{D,\,ms}$ for the ductility factor equal to 6 constantly or the damage index equal to 1.0 constantly is shown in Fig. 8. The mean $R_{D,\,seq}/R_{D,\,ms}$ are

within [0.82, 0.96] on site class B, while the mean $R_{D,\,seq}/R_{D,\,ms}$ are within [0.81, 0.96] on site class C. The aftershock ground motions with γ=1.0 would decrease the R_D factor at a level of < 20%. The R_D subjected to sequence-type ground motions is always less than that of mainshock ground motions, indicating that the strength demand of sequence-type ground motions is greater than that of mainshock ground motions. The effect of aftershock is significant in this case.

For the same damage index, the mean $R_{D,\,seq}/R_{D,\,ms}$ is insensitive to ductility factor. It indicates that the aftershock ground motion has similar effects on the R_D for different ductility factors. For the same ductility factor, the values of $R_{D,\,seq}/R_{D,\,ms}$ have little difference for various damage index except for D=0.1. The value of the mean $R_{D,\,seq}/R_{D,\,ms}$ for D=1 is quite larger than other values of D. This is because the systems remains in elastic region when D=0.1, and the cumulative damage is so small that can be ignored. In this case, the R_D is mainly depending on the historical maximal displacement, so the difference between $R_{D,\,seq}$ and $R_{D,\,ms}$ is subtle, as shown in Fig. 8a and c.

To study the influences of the intensity of sequence-type ground motions, the mean $R_{D,\,seq}/R_{D,\,ms}$ with different values of γ are analyzed. The mean $R_{D,\,seq}/R_{D,\,ms}$ of SDOF systems with μ=6 and D=1.0 subjected to sequence-type ground motions are shown in Fig. 9. It is obviously indicate that the mean $R_{D,\,seq}/R_{D,\,ms}$ decrease with
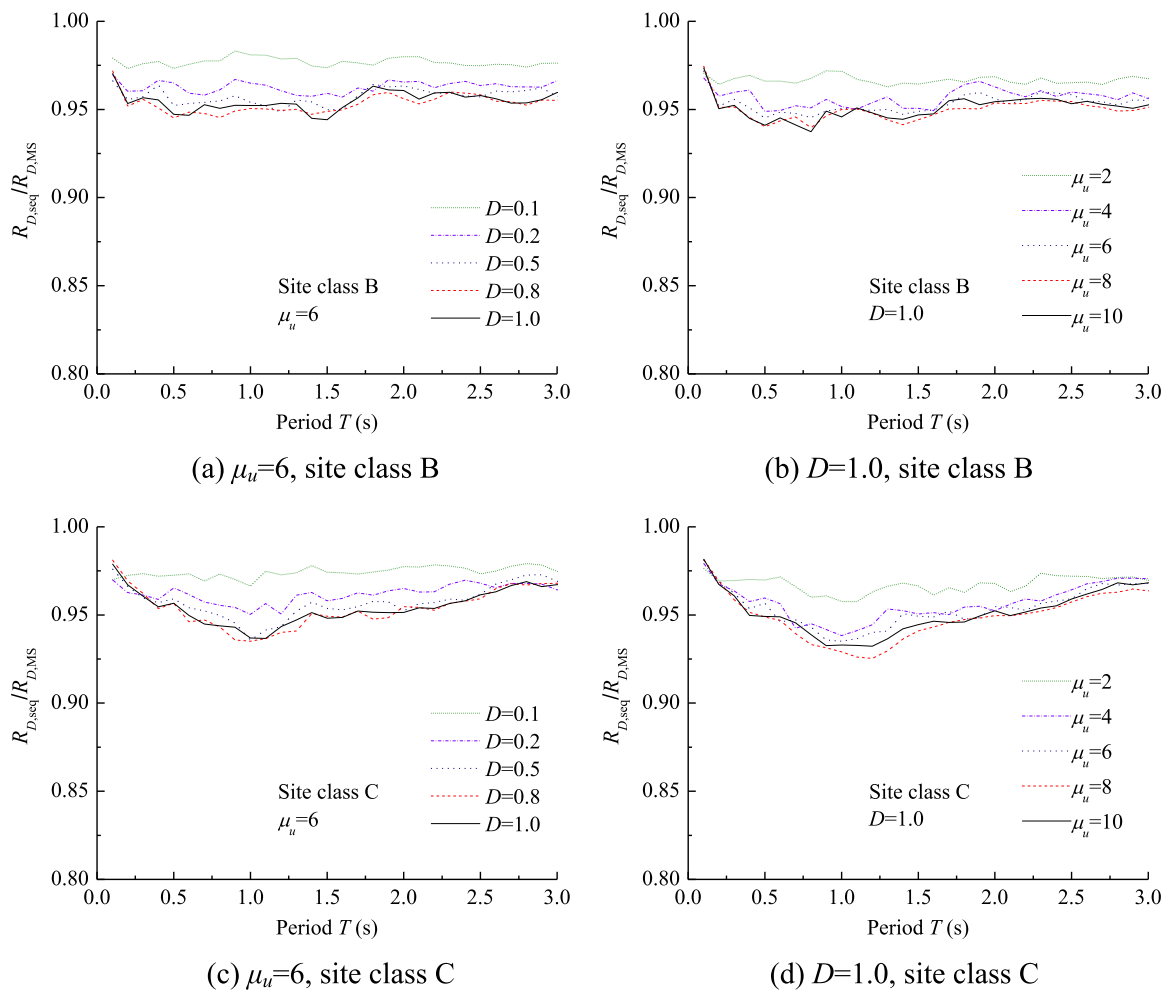
(a) μ_u=6, site class B

(b) D=1.0, site class B

(c) μ_u=6, site class C

(d) D=1.0, site class C

Fig. 7. The mean $R_{D,\text{seq}}/R_{D,\text{ms}}$ with the γ=0.5. (a) μ_u=6, site class B (b) D=1.0, site class B (c) μ_u=6, site class C (d) D=1.0, site class C.

the increase of γ. The effect of aftershock ground motion on the systems in short period region is greater than that on the systems in medium-long period region. Take mean $R_{D,\ seq}/R_{D,\ ms}$ of sequence-type ground motions with γ=1.5 as the example, the values of mean $R_{D,\ seq}/R_{D,\ ms}$ is smaller than 0.7 in the short period region while the values of mean $R_{D,\ seq}/R_{D,\ ms}$ is larger than 0.8 in the medium-long period region; That is to say, the R_D factor decrease by more than 30% in the short period region and less than 20% in the medium-long period region when the systems subjected to the aftershock ground motions with γ=1.5.

From the discussion above, the influence of aftershock on the R_D factor are related to the period of the system, the damage index and the intensity of aftershock. Besides, the damage of structures subjected to sequence-type ground motions is severer than that of structures subjected to mainshock ground motions due to the cumulative damage caused by aftershock. Therefore, the yield strength demand of sequence-type ground motions is greater. And the higher the intensity of aftershock is, the greater the yield strength demand is needed.

### 5.2. Effect of site conditions on the R_D spectra

The influence of site conditions on R_D spectra can be seen in Figs. 3 and 4 where mean R_D spectra are plotted for system subjected to sequence-type ground motions recorded on site class B and site class C. As shown in these figures, the R_D spectra on the two site condition

have the similar tendency in all period range.

For the convenience of comparison, the ratio between the R_D spectra for site class B and the R_D spectra for site class C are calculated and the results are plotted in Fig. 10. It is shown that site class B exhibits lower R_D values in the short period (< 1.0 s), while exhibiting higher R_D values in the long period (1.0–3.0 s). This phenomenon implies that the neglecting of site condition effect will lead to a certain overestimation of inelastic strength demand in the short period (< 1.0 s). The R_D spectra on site class C exhibit an opposite trend. However, the errors are within 10% for different ductility levels and damage indices. Thus, the influence of site condition on the R_D spectra can be neglected. The R_D is just a reduction factor from elastic spectra to inelastic spectra. Besides, the effect of site condition on the R_D spectra does not reflect its effect on elastic spectra and inelastic spectra.

5.3. Effect of post-yield stiffness on the R_D spectra

To study the influence of post-yield stiffness ratio H on R_D factor, two levels (5% and 10%) of post-yield stiffness ratio are selected to compare the influence. For the convenience of comparison, the ratio between the R_D spectra of different post-yield stiffness ratio and the R_D spectra of elastic-perfectly plastic are computed and the results are listed in Fig. 11. The R_D factor of elastic-perfectly plastic is 0.9–1.0 times of the R_D factor of 5%
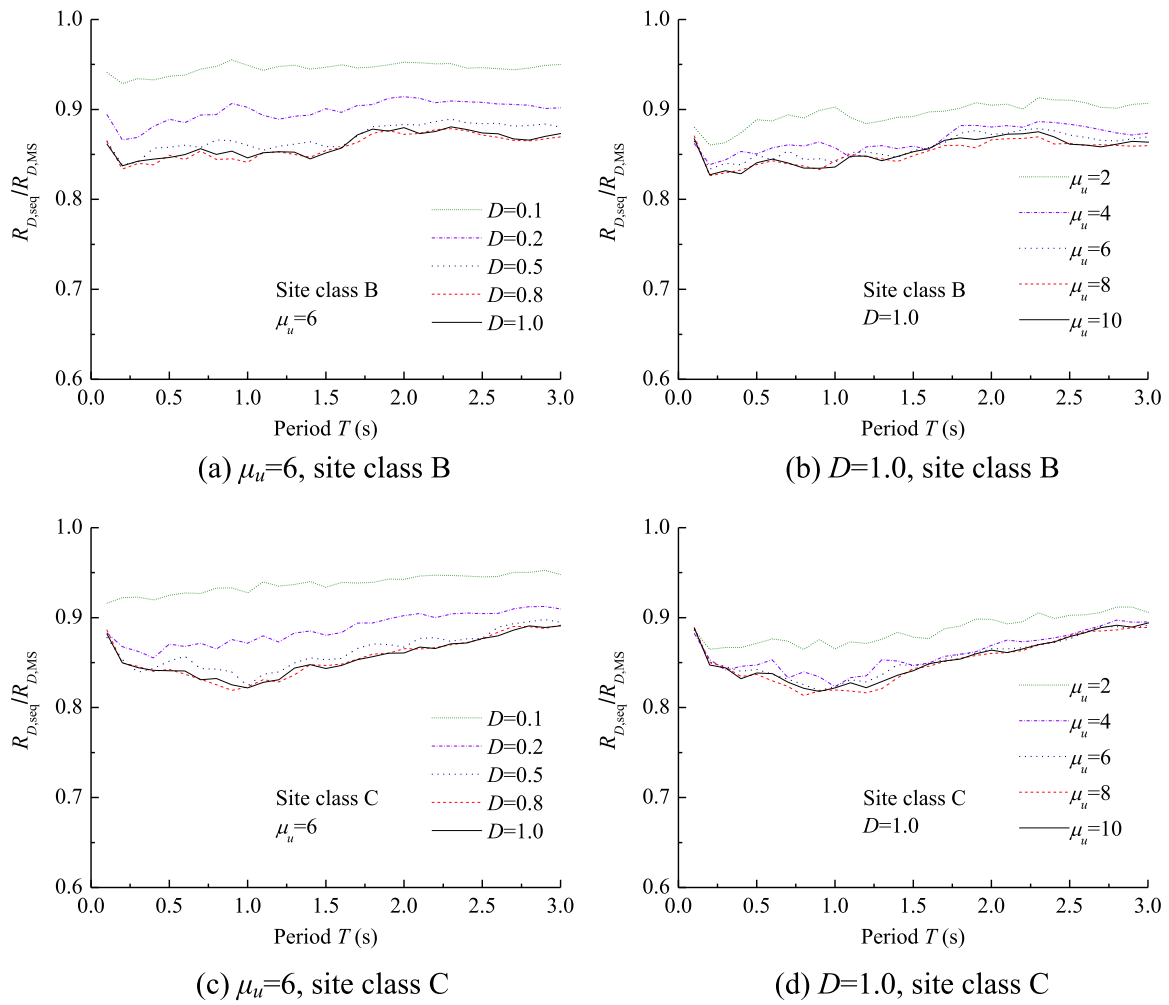
(a) μ_u=6, site class B

(b) D=1.0, site class B

(c) μ_u=6, site class C

(d) D=1.0, site class C

Fig. 8. The mean $R_{D,\mathrm{seq}}/R_{D,\mathrm{ms}}$ with the γ=1.0. (a) μ_u=6, site class B (b) D=1.0, site class B (c) μ_u=6, site class C (d) D=1.0, site class C.

(a) Site class B
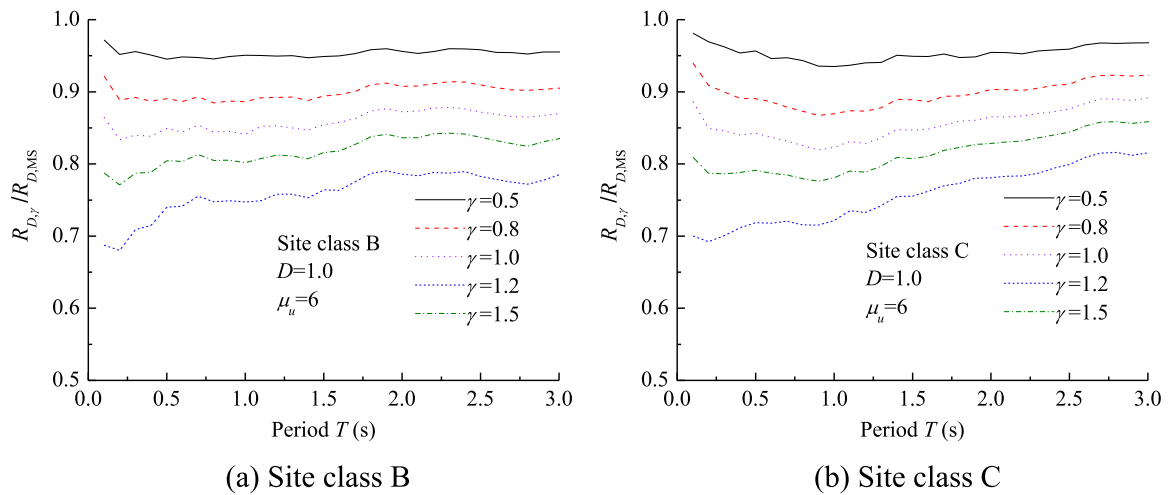
(b) Site class C

Fig. 9. The mean $R_{D,\mathrm{seq}}/R_{D,\mathrm{ms}}$ with different γ, μ_u=6, D=1.0. (a) Site class B (b) Site class C.

post-yield stiffness ratio, while the R_D factor of 5% post-yield stiffness ratio is 0.95−1.0 times of the R_D factor of 10% post-yield stiffness ratio. The results indicate that the increase of this ratio leads to a slightly increase of R_D factor, but not the major influence factor.

5.4. Effect of damping on the $\mathrm{R_D}$ spectra

To study the effect of damping, the R_D of systems with damping ratio ζ=0.02 and ζ=0.10 is calculated. The R_D of structures with damping ratio ζ=0.02 and ζ=0.10 is normalized by the R_D of structures
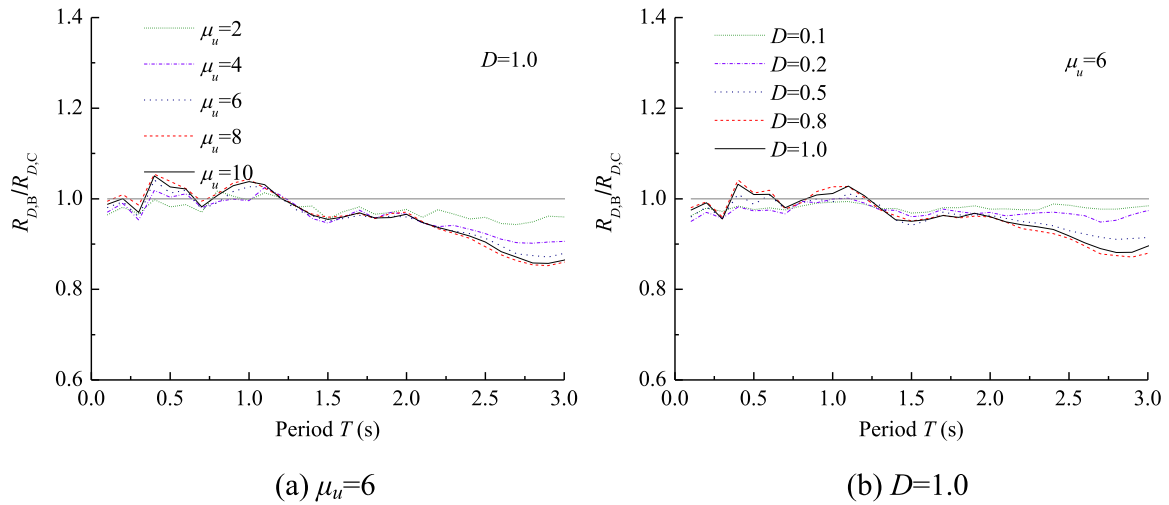
Fig. 10. Influence of site class on R_D factor, γ=0.5. (a) μ_u=6 (b) D=1.0.

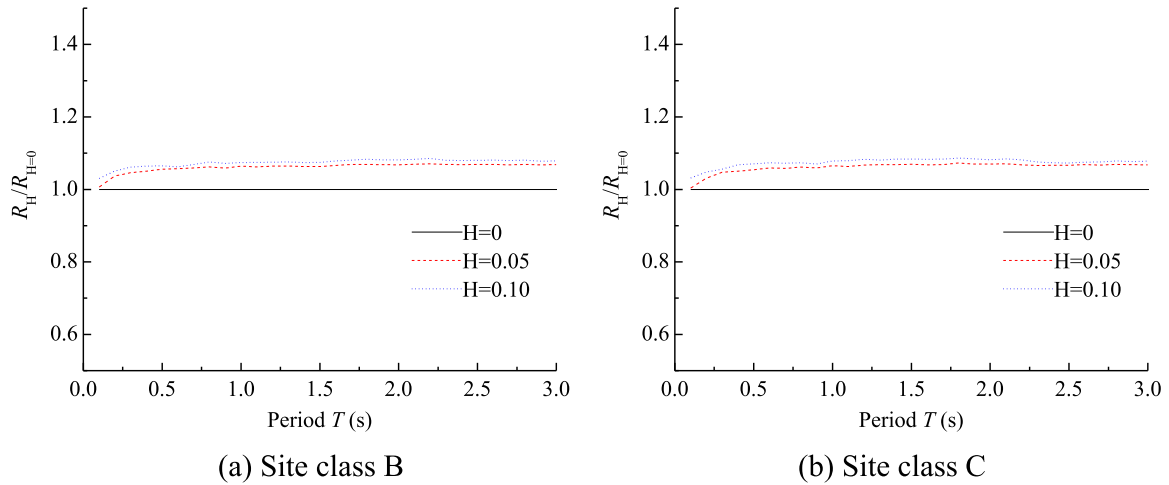**Fig. 11.** Influence of post-yield stiffness ratio on R_D factor, γ=0.5, μ_u=6, D=1.0. (a) Site class B (b) Site class C.

with ζ=0.05 for sequence-type ground motions with γ=0.5, as shown in Fig. 12.

It is evident that the decrease of damping ratio always results to increase of R_D factor by various extents. For elastic structures, the input energy is dissipated by the structural damping; for inelastic structures, the input energy is dissipated by the structural damping and hysteretic energy. The damping has a significant influence on the elastic structures and a less effect on the inelastic structures. Thus, the R_D factor decreases with the increase of structural damping.

Take the R_D of ζ=0.05 as the benchmark, the influence of damping is commonly within 20% and 15% for ζ=0.02 and ζ=0.10 respectively. With the decrease of damage index, the corresponding R_D of ζ=0.02 or ζ=0.10 is approaching to the R_D of ζ=0.05.

6. Proposed R_D spectra and comparison with existing R_μ & R_D spectra

6.1. Proposed empirical expressions for R_D spectra

For practical purpose, the overall mean R_D curves are desired to using a unified expression because of the similarity shape of mean R_D for different grouping of parameters. Modification coefficients can be employed to incorporate for special condition. Based on the observations above, three factors, which have a significant effect on R_D spectra,

are considered to conduct regression analysis. Then, the simplified expression of R_D is the function of period T, damage index D and ductility μ_u, that is

$$R_D = R_D(T, D, \mu_u) \tag{6}$$

Furthermore, the simplified expression of R_D must satisfy the following boundary limits:

(1) When the period of structure is close to zero, the corresponding yield displacement tends to zero and a small reduction of elastic strength leads to very large ductility. Thus very stiff structures should be design as elastic system:

$$R_D(T \rightarrow 0, D, \mu_u) = 1 \tag{7}$$

(2) For a structure, the damage index D=0 means that the structure subjected to ground motions suffers no damage, so the structure will stay elastic stage without reduction of the strength:

$$R_D(T, D = 0, \mu_u) = 1 \tag{8}$$

(3) For a structure, the ductility μ_u=1 means that the structure will stay elastic stage without reduction of the strength:

$$R_D(T, D, \mu_u = 1) = 1 \tag{9}$$

(4) In large period range, R_D will close to a constant value, denoted as

(a) μ_u=6, site class B

(b) D=1.0, site class B

(c) μ_u=6, site class C
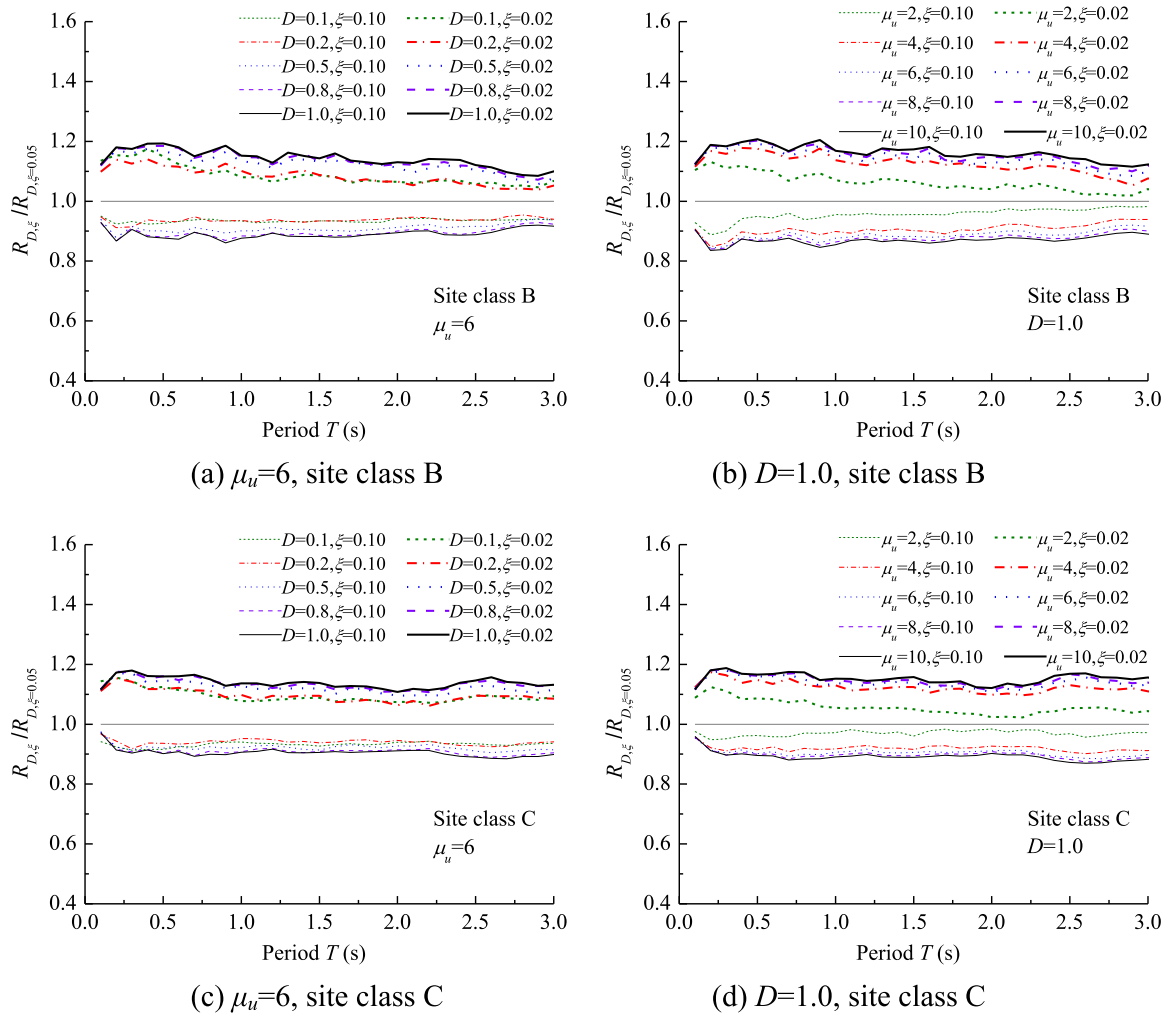
(d) D=1.0, site class C

Fig. 12. The mean normalized R_D of all sequence-type ground motions with γ=0.5. (a) μ_u=6, site class B (b) D=1.0, site class B (c) μ_u=6, site class C (d) D=1.0, site class C.

Table 3
The value of $a_0 \sim a_4$.

Para.	a_0	a_1	a_2	a_3	a_4
Site class B	26.84	37.68	13.76	1.28	4.99
Site class C	51.88	−13.88	13.44	4.76	−1.35

$\widetilde{R}_D$, which is a function of damage index and ductility.

$$R_D(T \rightarrow \infty, D, \mu_u) \rightarrow \widetilde{R}_D \tag{10}$$

Based on all the above assumptions, the following equation for the mean R_D spectra is obtained by regression analysis:

$$R_D = 1 + \frac{D(\mu - 1)(a_0 T + a_1 T^2)}{(\mu + a_2)(1 + a_3 T + a_4 T^2)} \cdot \frac{1}{0.87 + 0.08 e^\gamma} \tag{11}$$

where a_0, a_1, a_2, a_3 and a_4 are regression parameters depending on the site class, post-yield stiffness, the values of the parameters are listed in Table 3.

The predicted R_D spectra using Eq. (11) are compared with the actual mean spectra with the statistical results and the sequence

ground motions with γ=0.5, as shown in Figs. 13 and 14. A good match is observed for all damage indices and ductility classes.

6.2. Comparison of the proposed R_D spectra with existing R_μ & R_D spectra

As mentioned before, the previous relationships R_μ-μ-T represents that the ductility-based strength reduction factor is related to ductility and period with the ultimate limit state. The damage-based strength reduction factor is related to period, ductility and damage index, donated as R_μ-μ-D-T relationship. In order to compare the difference between the R_μ and the R_D, the R_D spectra with the ultimate limit state D=1.0 and the R_μ spectra are draw in Fig. 15. Generally, the R_D spectra and the R_μ spectra exhibit similar trends. The R_D spectra are always lower than the R_μ spectra at same ductility and soil condition. Meanwhile, when the ductility factor is small, the difference between
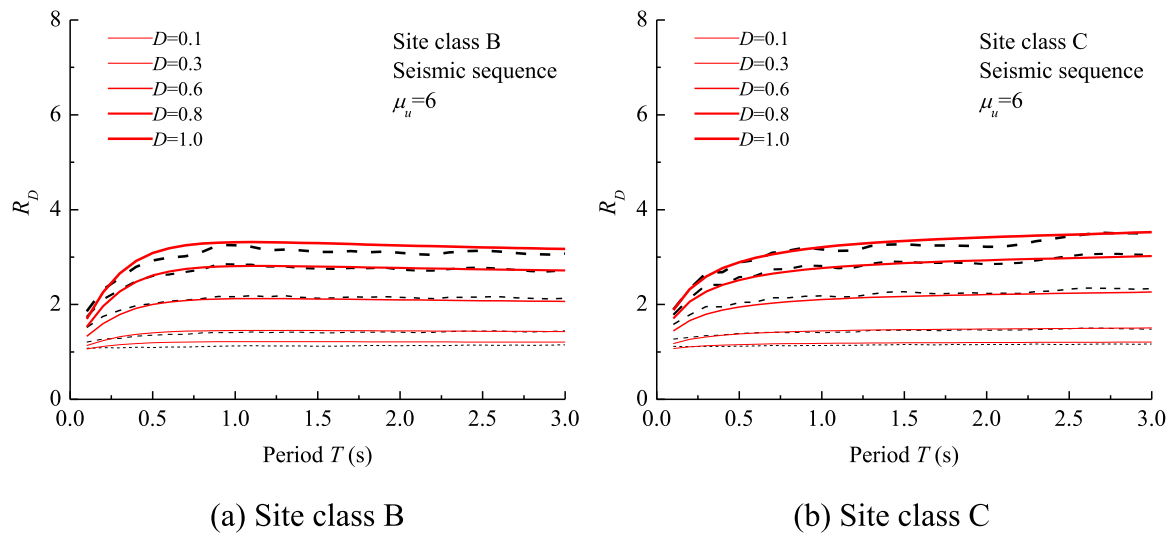
(a) Site class B

(b) Site class C

Fig. 13. Comparison of the computed R_D spectra with the original spectra (μ_u=6, γ=0.5). (a) Site class B (b) Site class C.
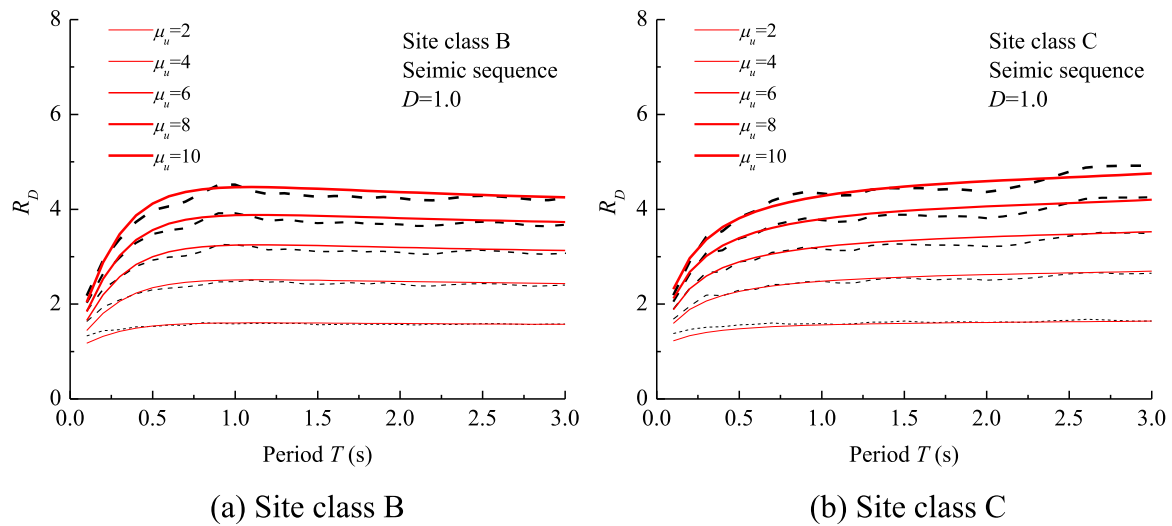

(a) Site class B

(b) Site class C

Fig. 14. Comparison of the computed R_D spectra with the original spectra (D=1.0, γ=0.5). (a) Site class B (b) Site class C.

the two is not obvious, but with the increase of the ductility factor, the difference becomes obvious. Comparing the strength reduction factor of sequence-type ground motion and aftershock ground motion, the difference is significant, indicating that the influence of aftershock cannot be ignored.

7. Conclusions

The primary purpose of this paper is to investigate the damage-based strength reduction factor R_D for sequence-type ground motions. The construction of R_D spectra for various damage index and ductility levels ensure a more rational determination of strength demand of inelastic systems, taking into account the cumulative damage with multiple performance targets. For the purpose, a statistical study of R_D factor was conducted. The R_D factors are computed for a series of elastic-plastic SDOF systems undergoing different levels of damage index and ductility factor subjected to a large number of sequence-type ground motions recorded on different site conditions. The influence of aftershock on R_D is specially studied. The following conclusion can be drawn

from this study.

The R_D factor is strongly dependent on the period of system in short period and approximately independent on the long period.

The difference between damage-based strength reduction factor R_D and damage-based strength reduction factor R_μ is significant, and the latter is 40% higher than the former in the long period for sequence-type ground motions. That is, the strength demand determined by R_D factor is greater than that determined by R_μ factor.

The influence of aftershock ground motion on R_D factor increases with the increase of intensity of the aftershock. The effect of aftershock ground motion with γ=0.5 on R_D factor can be negligible, while the aftershock ground motion with γ=1.5 can decrease the R_D with short period at a level of more than 25%. The effect of aftershock ground motion on R_D factor depend on the period, ductility factor, damage index and the intensity of the aftershock ground motion.

The proposed expression of the R_D is proposed as a function of period, damage index and ductility factor. The regression parameters are dependent on the site condition, post-yield stiffness ratio and the
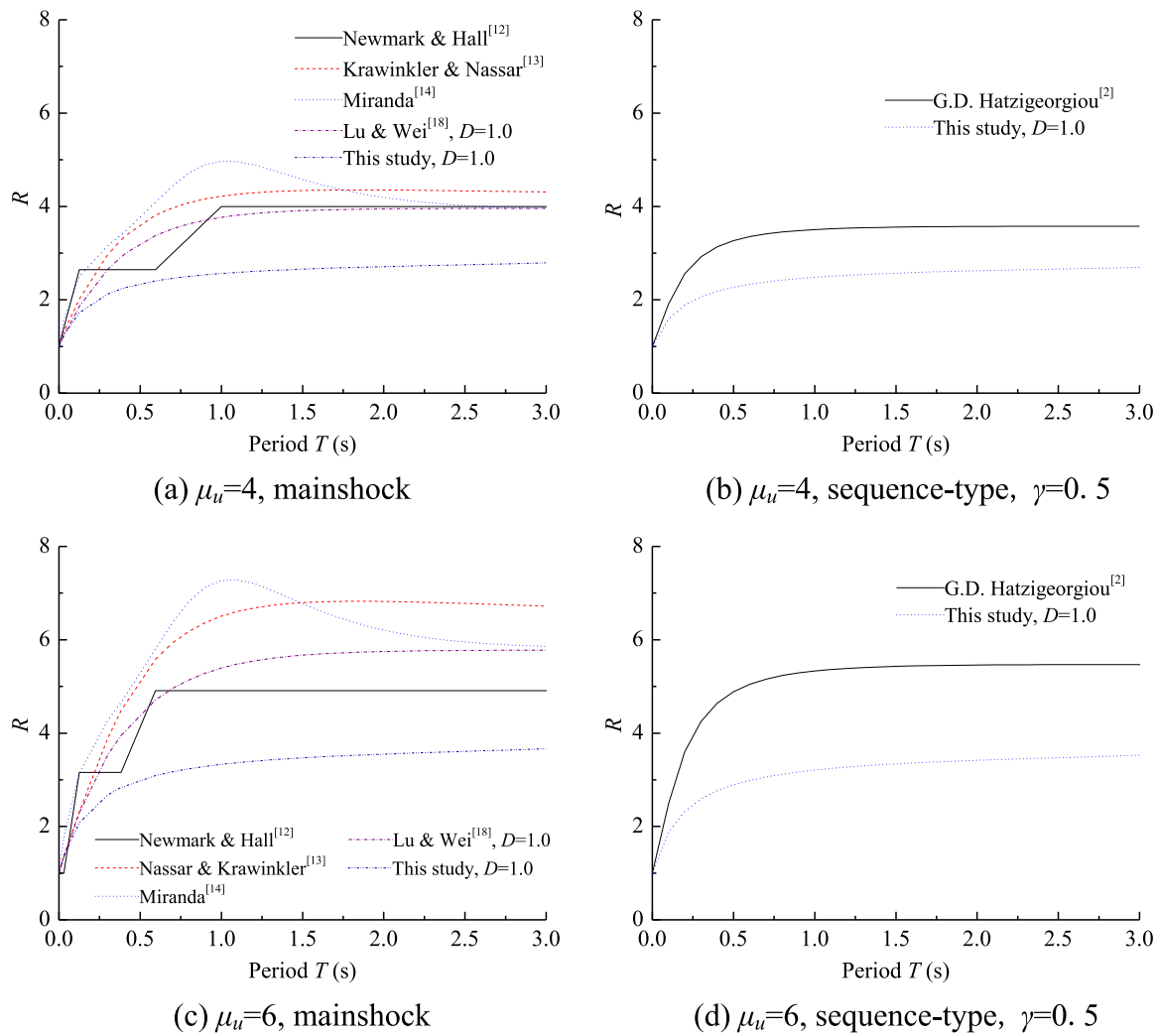
(a) $\mu_u=4$, mainshock

(b) $\mu_u=4$, sequence-type, $\gamma=0.5$

(c) $\mu_u=6$, mainshock

(d) $\mu_u=6$, sequence-type, $\gamma=0.5$

Fig. 15. Comparison of the proposed R_D spectra with the previous R_μ & R_D spectra, site class C. (a) $\mu_u=6$, mainshock (b) $\mu_u=6$, sequence-type (c) $\mu_u=4$, mainshock (d) $\mu_u=4$, sequence-type.

intensity of aftershock ground motion. The expression of the R_D can be used to easily determine the strength demand of inelastic systems in seismic design.

References

[1] Moon L, Dizhur D, Senaldi I, Derakhshan H, Griffith M, Magenes G, Ingham J. The demise of the URM building stock in Christchurch during the 2010 − 2011 canterbury earthquake sequence. Earthq Spectra 2014;30(1):253−76.

[2] Qu Z, Yang YQ. Seismic damages to owner-built dwellings in the 2015 earthquake sequence in Nepal. Earthq Eng Struct Dyn 2015;35(4):51−9.

[3] Hatzigeorgiou GD. Behavior factors for nonlinear structures subjected to multiple near-fault earthquakes. Comput Struct 2010;88(5):309−21.

[4] Zhai CH, Wen WP, Li S, Xie LL. The ductility-based strength reduction factor for the mainshock−aftershock sequence-type ground motions. Bull Earthq Eng 2015;13(10):2893−914.

[5] Zhai CH, Wen WP, Chen Z Z, Li S, Xie LL. Damage spectra for the mainshock-aftershock sequence-type ground motions. Earthq Eng Struct Dyn 2013;45(2):1−12.

[6] Hatzigeorgiou GD. Ductility demand spectra for multiple near- and far-fault earthquakes. Soil Dyn Earthq Eng 2010;30(4):170−83.

[7] Goda K, Taylor CA. Effects of aftershocks on peak ductility demand due to strong ground motion records from shallow crustal earthquakes. Earthq Eng Struct Dyn 2012;41(12):2311−30.

[8] Li Q, Ellingwood BR. Performance evaluation and damage assessment of steel frame buildings under main shock−aftershock earthquake sequences. Earthq Eng Struct Dyn 2007;36(3):405−27.

[9] Hatzigeorgiou GD, Liolios AA. Nonlinear behaviour of RC frames under repeated strong ground motions. Soil Dyn Earthq Eng 2010;30(10):1010−25.

[10] Newmark NM, Hall WJ. Seismic design criteria for nuclear reactor facilities. Report No 46, building practices for disaster mitigation. National Bureau of Standards; U. S. Department of Commerce; 1973. p. 209−236.

[11] Krawinkler H, Nassar AA. Seismic design based on ductility and cumulative damage demands and capacities. In: Fajfa P, Krawinkler H, editors. Nonlinear seismic analysis and design of RC buildings. Elsevier; 1992. p. 23−39.

[12] Miranda E. Site-dependent strength reduction factors. ASCE J Struct Eng 1993;119(12):3503−19.

[13] Fajfar P. Equivalent ductility factors, taking into account low-cycle fatigue. Earthq Eng Struct Dyn 1992;21(10):837−48.

[14] JeanW, LohC. Seismic demand for SDOF system based on structural damage control concept. In: Proceedings of the sixth east asia-pacific conference on structural engineering and construction. Taipei, Taiwan; 1998. p. 1633−38.

[15] Lu Y, Wei J. Damage-based inelastic response spectra for seismic design incorporating performance considerations. Soil Dyn Earthq Eng 2008;28(7):536−49.

[16] Amadio C, Fragiacomo M, Rajgelj S. The effects of repeated earthquake ground motions on the non-linear response of SDOF systems. Earthq Eng Struct Dyn 2003;32(2):291−308.

[17] Ruiz-García J, Negrete-Manriquez JC. Evaluation of drift demands in existing steel frames under as-recorded far-field and near-fault mainshock−aftershock seismic sequences. Eng Struct 2011;33(2):621−34.

[18] PEER strong motion database. Available online at: ⟨http://ngawest2.berkeley.edu/

⟩; 2014.

[19] Strong-motion seismograph networks (K-NET, KiK-net). Available online at: ⟨http://http://www.kyoshin.bosai.go.jp/⟩; 2016.

[20] Hatzigeorgiou GD, Beskos DE. Direct damage-controlled design of concrete structures. ASCE J Struct Eng 2007;133(2):205–15.

[21] Yue J, Qian J, Beskos DE. A generalized multi-level seismic damage model for RC framed structures. Soil Dyn Earthq Eng 2016;80(1):25–39.

[22] Park YJ, Ang AH-S. Mechanistic seismic damage model for reinforced concrete. ASCE J Struct Eng 1985;111(4):722–39.

[23] KunnathSK, ReinhornAM, LoboRF. IDARC version 3.0: a program for the inelastic

damage analysis of reinforced concrete structures. Technical report no. NCEER-92-0022. National Center for Earthquake Engineering Research, State University of New York at Buffalo; 1992.

[24] Negro P. Experimental assessment of the global cyclic damage of R/C structures. J Earthq Eng 1997;1(3):543–62.

[25] Building Seismic Safety Council (BSSC). Prestandard and commentary for seismic rehabilitation of buildings. Report. FEMA-356. Washington, DC: Federal Emergency Management Agency; 2000.

[26] PriestleyMJN. Performance based seismic design. In: Proceedings of the 12th world conference on earthquake engineering. Auckland, New Zealand; 2000.